EPJ Web of Conferences **191**, 05005 (2018) https://doi.org/10.1051/epjconf/201819105005
QUARKS-2018

Relaxation to equilibrium and EOS in ultra-relativistic heavy-ion collisions

E. Zabrodin[1,2,3,*] and L. Bravina[1]

[1]Department of Physics, University of Oslo, PB 1048 Blindern, Oslo, Norway
[2]Skobeltsyn Institute of Nuclear Physics, Moscow State University, RU-119991 Moscow, Russia
[3]National Research Nuclear University "MEPhI" (Moscow Engineering Physics Institute), Kashirskoe highway 31, Moscow, RU-115409, Russia

Abstract. We study relaxation to equilibrium of hot and dense hadron-string matter produced in the central zone of central heavy-ion collisions at energies 11.6AGeV $\leq E_{lab} \leq$ 160AGeV. Two microscopic transport models, UrQMD and QGSM, are employed. The analysis is performed for the central cubic cell with volume $V = 125\,\mathrm{fm}^3$. To check how close the system is to the equilibrium, its hadron yields and hadron energy spectra are compared with those of the statistical model of ideal hadron gas. For all collision energies it was found that the matter in the cell was approaching the equilibrium state, which lasted about 10 - 20 fm/c. After that the matter became very dilute and the thermal contact between the hadrons was lost. Equation of state is well fitted to linear dependence $P/\varepsilon = a = c_s^2$, where the square of the sonic velocity c_s^2 increases from 0.12 at $E_{lab} = 11.6$ AGeV to 0.145 at $E_{lab} = 160$ AGeV. These results are valid also for very early times of the system evolution when the matter is still out of equilibrium. Together with the isentropic expansion, the linear dependence of P on ε supports the application of hydrodynamic description to early stages of heavy-ion collisions.

1 Introduction

Hypothesis of local or even global equilibrium emerging in a system of particles produced in hadronic or nuclear collisions at (ultra)relativistic energies was utilized by Fermi in [1]. It was the first attempt to apply the statistical model (SM) for the description of multiparticle processes in high energy reactions. Almost immediately it was realized that the system of strongly interacting particles should expand and cool down before the hadron freeze-out. Landau employed this circumstance in his famous hydrodynamic model [2, 3] of multiparticle production. Nowadays, the sophisticated hydrodynamic models are very popular tools for the description of not only $A + A$, but also pA and even pp collisions at high energies. Note, that the system of equations describing the evolution of even a perfect fluid is incomplete. We have five equations: $\partial_\mu T^{\mu\nu} = 0$, $u_\mu u^\mu = 1$, where $T^{\mu\nu}$ is the energy-momentum tensor and u_μ is the 4-velocity. The number of variables, however, is six: four components of u_μ, energy density ε and pressure P. To made the system of equations complete Landau picked up the equation of state (EOS) of gas of ultrarelativistic particles, $P = \varepsilon/3$. This explicitly

*e-mail: eugen.zabrodin@fys.uio.no

implies that the expanding fireball is in equilibrium. But the rate of relaxation of hot and dense matter ("the boiling liquid of operators", according to Pomeranchuk) to equilibrium state was unknown. Later on Bjorken in [4] postulated that equilibration took place within the proper time $\tau = \sqrt{t^2 - z^2} \approx 1$ fm/c. This estimation looks a bit conservative now, and modern hydrodynamic models often employ $\tau_{equil} \approx 0.5$ fm/c or even shorter times as initial condition. On the other hand, there is a big group of Monte Carlo microscopic transport models which do not rely on the assumption of local or global equilibrium. These models are also successfully used to describe relativistic hadronic and heavy-ion collisions. Therefore, it was very tempting to check the relaxation of hadron-string matter in these models to the equilibrium state. To our best knowledge, the first rigorous attempt was done in [5] within the framework of ultra-relativistic quantum molecular dynamics (UrQMD) model [6, 7]. Later on, we checked the relaxation to equilibrium in Monte Carlo realization [8, 9] of the quark-gluon string model (QGSM) [10] as well.

In contrast to stationary case, such as lattice QCD calculations, the system produced in relativistic heavy-ion collisions is an open one. It expands, most energetic particles can leave it freely, and both energy density and particle composition are continuously changing. In order to decide, whether or not the system is in the vicinity of equilibrium, we have to compare the hadron abundances and energy spectra to those provided by the statistical model of ideal hadron gas with essentially the same degrees of freedom (i.e., hadronic species) as in the tested microscopic model. To do this one has to define a certain volume inside the expanding fireball and then extract energy density ε, net baryon density ρ_B, and net strangeness density ρ_S. These parameters are inserted into a system of nonlinear equations, provided by the SM, to obtain temperature of the system T, and its baryon- and strangeness chemical potentials, μ_B and μ_S, respectively. After that it is possible to compare yields and energy distributions of hadrons in the tested volume to those in the SM.

The paper is organized as follows. Section 2 describes the basic features of two models, UrQMD and QGSM, employed for our analysis. Statistical model of ideal hadron gas is described in Sect. 3. Relaxation of hot and dense hadron matter to thermal and chemical equilibrium in a stationary central cell and in a cell of growing volume is studied in Sect. 4. Equation of state is extracted also. Conclusions are drawn in Sect. 5.

2 Basic features of microscopic transport models

Both UrQMD [6, 7] and QGSM [8, 9] are Monte Carlo event generators designed for description of relativistic hh, hA and $A + A$ interactions. The multiparticle production takes place via formation and fragmentation of specific colored objects, strings, stretching uniformly between the quarks, diquarks, and their antistates. The string tension is about $\kappa \approx 1$ fm/c, and strings break into hadrons via the Schwinger-like mechanism of (di)quark-anti(di)quark formation. However, both mechanisms of the string formation and string fragmentation in the models are different.

There are two possible methods of string excitation. UrQMD employs the longitudinal excitation of strings which is characteristic for all Lund-based string models [11]. Here the mass of the string arises from the momentum transfer, and the strings are stretching between the constituents belonging to the same hadron. QGSM utilizes the color exchange mechanism [10], in which the constituents at the string ends belong to different hadrons. The variety of subprocesses in the latter case is much richer compared to the longitudinal excitation. For the string fragmentation process the string models utilize three possible schemes. The first scenario, suggested by Lund [11], implies that the string always splits on a sub-string and a particle on a mass shell at the end of the fragmenting string. This option is realizes in UrQMD. The second scheme splits the string into two sub-strings according to the area law

[12]. The third option is the Field-Feynman mechanism [13], where the fragmentation takes place independently from both ends of the string. This scenario is employed in QGSM.

Both models utilize available experimental information, such as hadron cross sections, resonance widths and decay modes. For the description of hadron-nucleus and nucleus-nucleus collisions hadronic cascade is used. Particle propagation between the collisions is governed by Hamilton equations of motion. To obey the uncertainty principle, newly produced particles can interact only after the certain formation time. Pauli principle is implemented by blocking the final state if the outgoing phase space is already occupied.

3 Statistical model of ideal hadron gas

To determine the thermodynamic characteristics of system of hadrons which is in chemical and thermal equilibrium one has to know just three parameters, namely T, μ_B, μ_S. Then, the particle distribution functions of i-th hadron species with mass m_i, momentum p_i and energy $E_i = \sqrt{p^2 + m_i^2}$ read (recall, that $\hbar = c = k_{\rm B} = 1$)

$$f(p_i, m_i) = \left[\exp\left(\frac{E_i - \mu_i}{T}\right) \pm 1\right]^{-1} \quad , \tag{1}$$

$$\mu_i = \mu_B B_i + \mu_S S_i \quad , \tag{2}$$

where B_i and S_i are baryon charge and strangeness of i-th hadron, respectively. Moments of the distribution functions provide us partial particle number density, n_i, energy density ε_i, and pressure P_i:

$$n_i = \frac{g_i}{(2\pi)^3} \int f(p, m_i) \mathbf{d^3p} \quad , \tag{3}$$

$$\varepsilon_i = \frac{g_i}{(2\pi)^3} \int E_i f(p, m_i) \mathbf{d^3p} \quad , \tag{4}$$

$$P_i = \frac{g_i}{(2\pi)^3} \int \frac{p^2}{3E_i} f(p, m_i) \mathbf{d^3p} \quad , \tag{5}$$

where g_i is the degeneracy factor. The entropy density reads

$$s_i = -\frac{g_i}{(2\pi)^3} \int f(p, m_i) \left[\ln f(p, m_i) - 1\right] \mathbf{d^3p} \quad . \tag{6}$$

The energy density ε, net baryon density ρ_B and net strangeness density ρ_S of the whole system are

$$\varepsilon = \sum_i \varepsilon_i(T, \mu_B, \mu_S) \quad , \tag{7}$$

$$\rho_B = \sum_i B_i \cdot n_i(T, \mu_B, \mu_S) \quad , \tag{8}$$

$$\rho_S = \sum_i S_i \cdot n_i(T, \mu_B, \mu_S) \quad . \tag{9}$$

If these parameters are the same as ε^{mic}, ρ_B^{mic} and ρ_S^{mic}, extracted from microscopic model calculations, the hadron spectra in the SM can be directly compared to the snapshot spectra of the tested volume of expanding fireball. This procedure is discussed in the next Section.

4 Relaxation to equilibrium and EOS

Choice of the tested volume. Relaxation of hot and dense matter to (local) equilibrium in microscopic transport models was studied in calculations of central gold-gold or lead-lead collisions in a broad energy span from $E_{lab} = 11.6$ AGeV to $\sqrt{s} = 200$ GeV in [5, 14–20]. Results of calculations show that net baryon density is not distributed uniformly between the remnants of colliding nuclei. Therefore, central cubic cell with volume $V = 5 \times 5 \times 5 = 125\,\mathrm{fm}^3$ was chosen. The tested volume should be neither too small and contain enough hadrons, nor too big in order to be uniform. Modifications of the volume have been also studied. First idea was to reduce the cell size to volume $V = 4 \times 4 \times 1\,\mathrm{fm}^3$ and study the equilibration in a relatively thin central layer. Another scenario assumed the division of the central area of heavy-ion collisions into many tiny cells with volume $V = 0.5 \times 0.5 \times 0.5\,\mathrm{fm}^3$ each. The tested volume was enlarged if the energy density in the inner cell was the same as that in the layer of outer cells, - the coarse-graining procedure. This procedure was employed together with the "standard" one in [21–24].

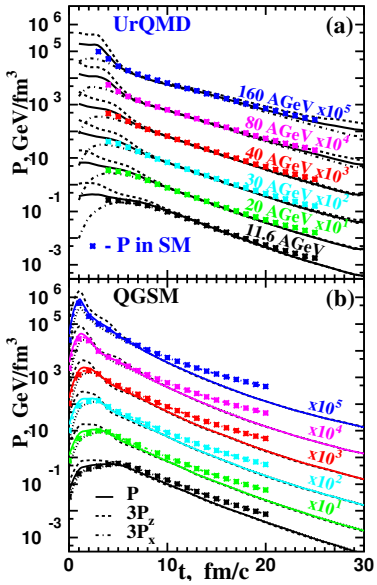

Figure 1. (a) Time evolution of pressure (solid lines) and triple pressure components in longitudinal (dashed lines) and transverse (dash-dotted lines) directions in the central cell of Au+Au collisions at energies from 11.6 AGeV to 160 AGeV in UrQMD calculations. Symbols indicate the SM calculations. (b) The same as (a) but for QGSM calculations.

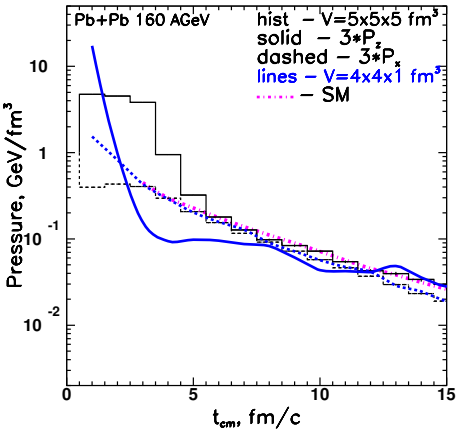

Figure 2. The same as Fig. 1 but for Pb+Pb collisions at 160 AGeV in UrQMD calculations for big cell with $V = 5 \times 5 \times 5$ fm^3 (black curves) and for small cell with $V = 4 \times 4 \times 1$ fm^3 (blue curves). Magenta dotted curve indicates SM calculations.

Check of pre-equilibrium conditions. Direct check of equilibrium conditions in the cell, i.e. correspondence of particle yields and energy spectra to those of the SM, from the very beginning of nuclear collision is time consuming and, therefore, not very efficient if the system is far from equilibrium. Other methods should be looked for. The pre-equilibrium conditions imply, for instance, (i) absence of significant collective flows in the cell, (ii) similarity of velocity distributions of hadrons in x-, y-, and z-directions, or (iii) isotropy of pressure

in transverse and longitudinal directions. The last method is quite quick. We calculate the diagonal elements of the pressure tensor in the cell with volume V according to the virial theorem

$$P_{\{x,y,z\}} = \frac{1}{3V} \sum_i \frac{p^2_{i,\{x,y,z\}}}{E_i} \quad . \tag{10}$$

Here $p_{i,(x,y,z)}$ are the momentum components of the i-th hadron, and E_i is its energy, respectively. Figure 1 displays hadronic pressures calculated in the transverse and longitudinal directions in the central cell with $V = 125\,\mathrm{fm}^3$ of central Au+Au collisions at six bombarding energies. The total pressures, obtained both in UrQMD and QGSM, are plotted onto the partial pressures together with the results calculated within the SM. The pressure convergence in both models occurs at $3\ \mathrm{fm}/c \le t \le 6\ \mathrm{fm}/c$. This time decreases with increasing energy of the collision. It was tempting to check the possibility of earlier pressure isotropization in a smaller cell with short z-face. The corresponding distributions are shown in Fig. 2 for central cell with $V = 4 \times 4 \times 1\,\mathrm{fm}^3$ in central Pb+Pb collisions at $E_{lab} = 160\,\mathrm{AGeV}$. One can see that the isotropy of pressure in the small cell takes place at the same rate as for "standard" big cell with $V = 125\,\mathrm{fm}^3$. It is worth noting that meson velocity distributions in transverse and longitudinal directions converge to equilibrium longer that that of baryons because of the longer formation times and smaller cross-sections for non-leading hadrons, such as pions and kaons [14, 23].

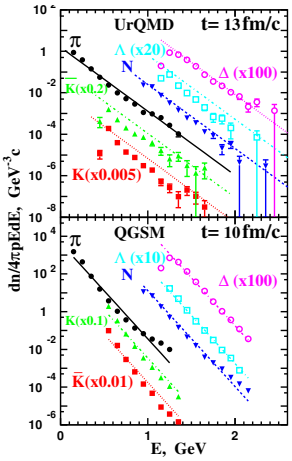

Figure 3. (Upper plot) Energy spectra of main hadron species in UrQMD calculations of Au+Au at 40 AGeV for central cell with $V = 125\ \mathrm{fm}^3$ at $t = 13\ \mathrm{fm}/c$. Lines indicate the fit to Boltzmann distribution. (Bottom plot) The same as upper one but for QGSM calculations at $t = 10\ \mathrm{fm}/c$.

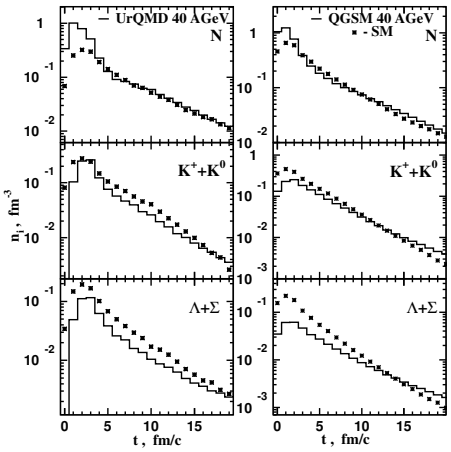

Figure 4. Hadron yields (histograms) in the central cell with $V = 125\ \mathrm{fm}^3$ of central Au+Au collisions at $E_{lab} = 40$ AGeV in UrQMD (left) and QGSM (right) calculations. Asterisks denote SM calculations.

Thermal and chemical equilibrium. After $t \approx 8 - 10\,\mathrm{fm}/c$, energy spectra and yields of hadronic species in the cell are very close to those given by the SM. Figure 3 shows the $dn/4\pi pEdE$ spectra of hadrons in the central cell in central Pb+Pb collisions at $E_{lab} = 40$ AGeV calculated within UrQMD at $t = 13\ \mathrm{fm}/c$, and within QGSM at $t = 10\ \mathrm{fm}/c$. We see that the spectra of different hadrons have the same slope within 10% of accuracy. Evolution

of particle abundances in the cell is displayed in Fig. 4. Results of microscopic model calculations are very close to predictions of the SM. One may conclude that hadrons in the cell are very close to the state of thermal and chemical equilibrium for a period of $10 - 15\,\mathrm{fm}/c$. At the late stage the matter in the cell becomes very dilute , and the (quasi)elastic collisions cannot maintain the thermal equilibrium anymore.

Equation of state. Landau hydrodynamic model [2] postulates that the expansion of relativistic fluid proceeds isentropically. But the cell is an open system, and its conditions are permanently changing. Despite of this difficulty, we can check the evolution of the entropy per baryon. The ratio s/ρ_B is presented in Fig. 5. Similar to the case of the pressure convergence, this ratio reaches the constant value (within 5% accuracy limit) already at $t \approx 3\,\mathrm{fm}/c$.

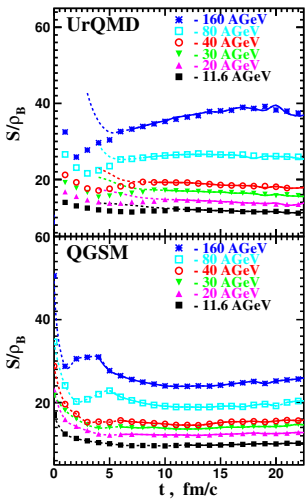

Figure 5. Entropy per baryon ratio (dashed lines) vs time in central cell with volume $V = 125\ \mathrm{fm}^3$ in UrQMD (upper plot) and QGSM (bottom plot) calculations of central Au+Au collisions at six different energies. Asterisks denote SM calculations.

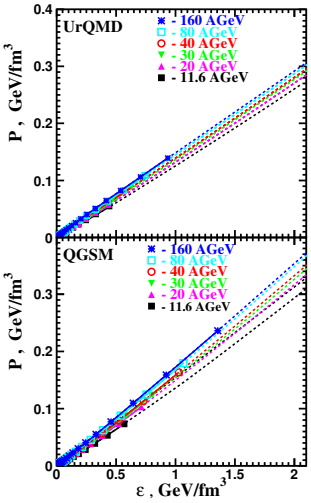

Figure 6. Time evolution of the pressure vs. energy density in the central cell with volume $V = 125\,\mathrm{fm}^3$ in UrQMD (upper plot) and QGSM (bottom plot) calculations of Au+Au collisions at six different energies. Symbols are related to equilibrium stage; the time step is $\Delta t = 1\,\mathrm{fm}/c$.

Finally, the equation of state should be examined. The well-known result for the gas of ultrarelativistic particles $P = \varepsilon/3$ means that the speed of sound is $c_s = 1/\sqrt{3}$ of the speed of light. As was shown in [25], the presence of resonances reduces the sonic speed to $c_s^2 \approx 0.14-0.15$. Time evolution of macroscopic pressures and energy densities, obtained from the SM fit to microscopic calculations of central heavy-ion collisions at different energies, is shown in Fig. 6. Dashed lines indicate the results related to both pre-equilibrium and equilibrium stages, whereas asterisks denote the $P(\varepsilon)$ in the cell after reaching the equilibrium. Time step is $\Delta t = 1\,\mathrm{fm}/c$. One can see that at any energies between $E_{lab} = 11.6\,\mathrm{AGeV}$ and 160 AGeV the EOS has remarkable linear dependence, $P = a\varepsilon$, where $a \equiv c_s^2$ varies from 0.12 to 0.145. - Note that the sonic velocity is almost the same for heavy-ion collisions at SPS and at RHIC energies, see e.g. [17]. - Together with the almost isentropic expansion of the matter in the cell, the latter result strongly supports the application of hydrodynamics to early stages of the fireball evolution, when the hadronic matter is not in chemical and thermal equilibrium [26].

5 Conclusions

Two different Monte Carlo transport models, UrQMD and QGSM, show that the hot and dense matter produced in the central area of central heavy-ion collisions at 11.6AGeV $\leq$ $E_{lab} \leq$ 160 AGeV reaches the state which is very close to the state of thermal and chemical equilibrium. The equilibration occurs at $t \approx 8 - 10$ fm/c and lasts for $10 - 15$ fm/c. After that the thermal contact between hadrons is lost.

The stage of pre-equilibrium, however, is reached already at $t \approx 3$ fm/c. From this time (i) pressure in the central cell becomes isotropic, (ii) expansion of matter in the cell proceeds with constant entropy per baryon ratio, and (iii) evolution of pressure with energy density has the same slope $dP/d\varepsilon$ as that in the total equilibrium. The equation of state is well described by linear dependence $P = a\varepsilon$, where $a = c_s^2$ varies from 0.12 at $E_{lab} = 11.6$ AGeV to 0.145 at $E_{lab} = 160$ AGeV. This EOS completes the system of hydrodynamic equations, thus favoring the idea that the hydrodynamic description under certain conditions can be applied to systems which are out of local equilibrium. In other words, extremely early equilibration may not be a necessary condition for applicability of hydrodynamic models of heavy-ion collisions.

Fruitful discussions with M. Bleicher, E. Boos, K. Bugaev and L. Csernai are gratefully acknowledged. This work was supported by the Norwegian Research Council (NFR) under grant No. 255253/F50 - "CERN Heavy Ion Theory". It was also performed in the framework of COST Action CA15213 "Theory of hot matter and relativistic heavy-ion collisions" (THOR).

References

[1] E. Fermi, Prog. Theor. Phys. **5**, 570 (1950)
[2] L.D. Landau, Izv. Akad. Nauk SSSR, Ser. Fiz. **17**, 51 (1953) 51 (in Russian)
[3] S.Z. Belenkij and L.D. Landau, Nuovo Cimento Suppl. **3**, 15 (1956)
[4] J.D. Bjorken, Phys. Rev. **D27**, 140 (1983)
[5] L.V. Bravina *et al.*, Phys. Lett. **B434**, 379 (1998)
[6] S.A. Bass *et al.*, Prog. Part. Nucl. Phys. **41**, 255 (1998)
[7] M. Bleicher *et al.*, J. Phys. **G25**, 1859 (1999)
[8] N.S. Amelin and L.V. Bravina, Sov. J. Nucl. Phys. **51**, 133 (1990)
[9] J. Bleibel, L.V. Bravina, E.E. Zabrodin, Phys. Rev. **D93**, 114012 (2016)
[10] A.B. Kaidalov, Surveys in High Energy Phys. **13**, 265 (1999)
[11] B. Andersson, G. Gustafson, B. Nilsson-Almqvist, Nucl. Phys. **B281**, 289 (1987)
[12] X. Artru, G. Menessier, Nucl. Phys. **B70**, 93 (1974)
[13] R.D. Field, R.P. Feynman, Nucl. Phys. **B136**, 1 (1978)
[14] L.V. Bravina *et al.*, J. Phys. **G25**, 351 (1999)
[15] L.V. Bravina *et al.*, Phys. Rev. **C60**, 024904 (1999)
[16] L.V. Bravina *et al.*, Nucl. Phys. **A661**, 600 (1999)
[17] L.V. Bravina *et al.*, Phys. Rev. **C63**, 064902 (2001)
[18] L.V. Bravina *et al.*, J. Phys. **G27**, 421 (2001)
[19] L.V. Bravina *et al.*, Nucl. Phys. **A698**, 383c (2002)
[20] L.V. Bravina *et al.*, Phys. Rev. **C62**, 064906 (2000)
[21] L.V. Bravina *et al.*, J. Phys. **G32**, S213 (2006)
[22] L.V. Bravina *et al.*, Int. J. Mod. Phys. **E16**, 777 (2007)
[23] L.V. Bravina *et al.*, Phys. Rev. **C78**, 014907 (2008)
[24] L.V. Bravina *et al.*, J. Phys. **G36**, 064065 (2009)
[25] E. Shuryak, Sov. J. Nucl. Phys. **16**, 220 (1973)

[26] Ph. Mota, T. Kodama, R.D. de Souza, J. Takahashi, Eur. Phys. J. **A48**, 165 (2012)